CHEMISTRY
A EUROPEAN JOURNAL

Molecular Recognition of Aminoglycoside Antibiotics by Bacterial Defence Proteins: NMR Study of the Structural and Conformational Features of Streptomycin Inactivation by *Bacillus subtilis* Aminoglycoside-6-adenyl Transferase

Francisco Corzana,[a] Igor Cuesta,[a] Agatha Bastida,*[a] Ana Hidalgo,[a] Montserrat Latorre,[a] Carlos González,[b] Eduardo García-Junceda,[a] Jesús Jiménez-Barbero,[c] and Juan Luis. Asensio*[a]

Abstract: The molecular recognition of streptomycin by *Bacillus subtilis* aminoglycoside-6-adenyl transferase has been analysed by a combination of NMR techniques and molecular dynamic simulations. This protein inactivates streptomycin by transferring an adenyl group to position six of the streptidine moiety. Our combined approach provides valuable information about the bioactive conformation for both the antibiotic and ATP and shows that the molecular recognition process for streptomycin involves a conformational selection phenomenon. The binding epitope for both ligands has also been analysed by 1D-STD experiments. Finally, the specificity of the recognition process with respect to the aminoglycoside and to the nucleotide has been studied.

Keywords: aminoglycoside antibiotics · bacterial resistance · molecular dynamics · molecular recognition · NMR spectroscopy

Introduction

Streptomycin was the first aminoglycoside to be discovered, in 1943. It has a three-ring structure (Scheme 1) comprising a highly substituted aminocyclitol ring (the streptidine moiety), linked to a modified ribose (α-L-streptose), linked in turn to an *N*-methyl-α-L-glucosamine residue. This molecule proved to be the first chemotherapeutic agent effective against *Mycobacterium tuberculosis*.[1] Its biological target is the bacterial 30S ribosomal subunit. X-ray determination of streptomycin in complexation with this ribosomal subunit has provided extremely detailed knowledge about the interactions that stabilize the drug–RNA complex.[2]

The emergence of bacterial resistance to the major classes of antibiotics has become a serious problem over recent years.[3] Acquired resistance to aminoglycoside antibiotics can occur through three different mechanisms: mutation of the ribosomal target, reduced permeability for the antibiotics, and enzymatic modification of the drugs, thus leading to inactivation. Therefore, different substitutions in the bacterial ribosomal proteins or RNA have been associated with the phenomenon of bacterial resistance.[4–9] Similarly, a reduced uptake of aminoglycosides may play a clinical role in decreased efficacy.[10,11] However, it is important to point out that the most prevalent source of clinically relevant resistance is through the third mechanism: the enzymatic inactivation of the drugs.[3,5,12,13] Enzymes involved in bacterial defence against aminoglycoside antibiotics can be broadly classified as *N*-acetyl transferases (AACs), *O*-adenyl transferases (ANTs), and *O*-phosphotransferases (APHs). It is evident that detailed knowledge of the structures of these enzymes and their interactions with the drugs should provide a framework to facilitate the rational design either of novel

[a] Dr. F. Corzana, I. Cuesta, Dr. A. Bastida, A. Hidalgo, M. Latorre, Dr. E. García-Junceda, Dr. J. L. Asensio
Instituto de Química Orgánica, CSIC
Juan de la Cierva 3, 28006 Madrid (Spain)
Fax: (+34) 91-564-4853
E-mail: iqoa110@iqog.csic.es

[b] Dr. C. González
Instituto de Química Física Rocasolano, CSIC
Madrid (Spain)

[c] Prof. Dr. J. Jiménez-Barbero
Centro de Investigaciones Biológicas, CSIC
Madrid (Spain)

Supporting information (Figures S1 to S9, showing details of the NMR analysis of the antibiotic and the nucleotides in the free and protein-bound states) for this article is available on the WWW under http://www.chemeurj.org/ or from the authors.

DOI: 10.1002/chem.200400941

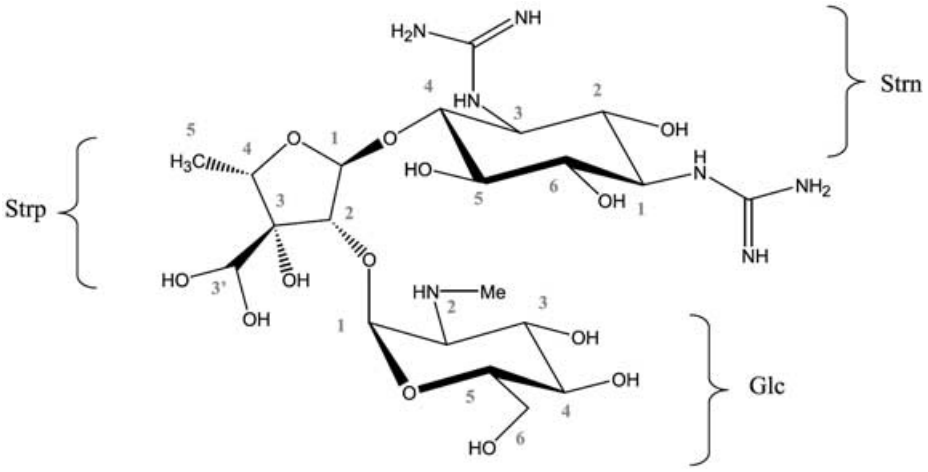

Scheme 1. Schematic representation of streptomycin, together with the numbering employed for the different sugar units.

aminoglycosides, not susceptible to modification, or of inhibitors of these enzymes, which could be administered in tandem with existing aminoglycosides. Unfortunately, detailed structural information about the enzymes involved in bacterial resistance is still sparse.

With respect to the ligand, it is well established that the three-dimensional structure of the oligosaccharides plays an essential role in their interaction with proteins and nucleic acids and thus determines their biological function.[14] In this sense, a proper understanding of the different factors governing sugar–protein interactions requires detailed knowledge of the three-dimensional structure of the oligosaccharide in both the free and the bound state. Although the two conformations are in most cases basically identical, this cannot be regarded as a general rule.[15] Thus, in those cases in which the ligand is flexible, the protein receptor may select only one of the structures present in solution. It might even stabilize high-energy conformations almost unpopulated in the free state.

Here we analyse the molecular recognition of streptomycin (Scheme 1) by *Bacillus subtilis* 6-*O*-adenyl-transferase (ANT(6)), a 37.5 kD protein involved in bacterial resistance against aminoglycosides, by a combination of experimentally measured NMR data and molecular dynamics and mechanics calculations. *O*-Adenyl transferases (ANTs) catalyse the transfer of an adenyl group from ATP to a hydroxy function on the antibiotic, thus leading to a sharp decrease in the drug affinity for its target RNA. More specifically, ANT(6) modifies position six of the streptidine moiety in streptomycin.[16] It is important to bear in mind that no detailed structure for any 6-*O*-adenyl-transferase has yet been solved either by X-ray or by NMR methods. Thus, as a first step in our efforts towards better understanding of the structural requirements for drug–enzyme interaction, we have analysed the conformational behaviour of streptomycin in both the free and the protein-bound states by NOESY and TR-NOESY/TR-ROESY experiments, respectively. In addition, the protein-bound structure of AMP has been determined. The recognition epitope for both the antibiotic and the nucleotide has also been analysed by STD (saturation transfer difference) experiments. Finally, the enzyme specificity with respect to the antibiotic and nucleotide has been studied.

Results and Discussion

The free state—conformational analysis of streptomycin in solution: In order to analyse the solution structure of streptomycin experimentally, selective 1D-NOE (one-dimensional nuclear Overhauser effect) experiments (Figure 1) were carried out at 318 K and pH 7.0 at 500 MHz. The streptidine signals are characterised by a large degree of overlap under these experimental conditions, so 800 MHz experiments (NOESY, TOCSY, HMQC) spectra were also performed (Figure S1 a) in order to assign all the structurally relevant NOEs unambiguously. In addition, ^3J values were measured for the two sugar units (glucose and streptose). Experimentally determined distances were derived from the corresponding NOE build-up curves[19] (see Figure S2 in the Supporting Information and the Experimental Section). To obtain an experimentally derived ensemble, 80 ns MD-tar (molecular dynamics with time-averaged restraints)[20] simulations (in vacuo, $\varepsilon = 80$) were carried out by inclusion of the experimental distances and the $J_{H1,H2}$ value corresponding to the streptose unit as time-average restraints, with the AMBER 5.0 program.[21] In addition, 20 ns unrestrained MD simulations were performed in the presence of explicit TIP3P[22] water and counter-ions for purposes of comparison. Table 1 shows the relevant NOE-derived distances and J values, together with those obtained from unrestrained and MD-tar simulations. The corresponding ϕ/ψ distributions for both glycosidic linkages are shown in Figure 2 a. The main conclusions obtained from this analysis can be summarised as follows:

- Both glycosidic linkages are characterised by the presence of two major conformations (labelled as A/B and A′/B′ for the Strp/Strn (Strp = streptose, Strn = streptidine) and Glc/Strp (Glc = glucose) bonds, respectively, in Figure 2 a).
- The conformational fluctuations around the two glycosidic linkages are strongly correlated. In fact, A→B or B→A transitions for the Strp/Strn linkage are in most cases accompanied by A′→B′ or B′→A′ transitions, respectively, for the Glc/Strp bond, as indicated in Figure S3 in the Supporting Information. In conclusion, the streptomycin solution structure is characterised by the presence of two main conformational families, dubbed

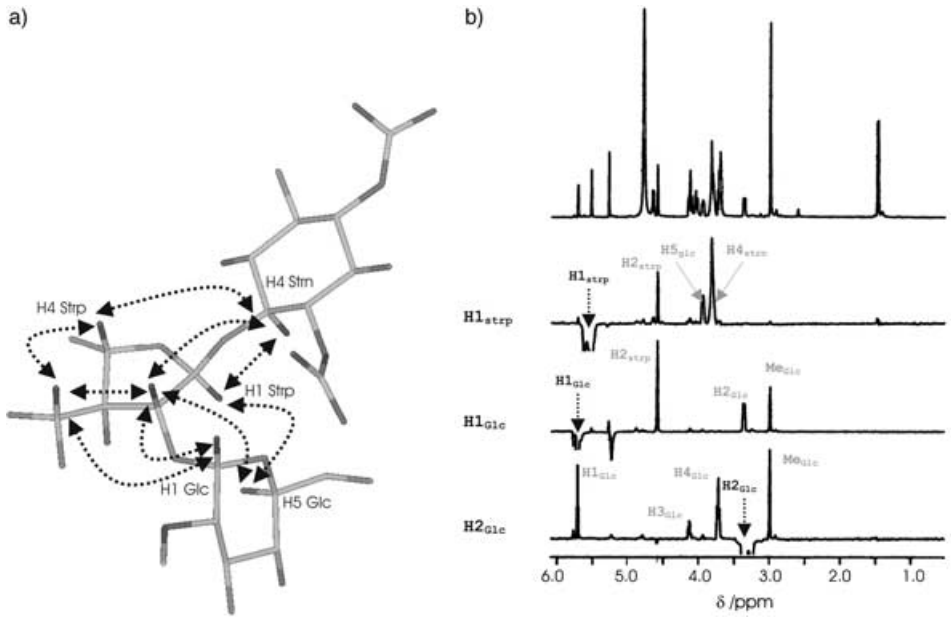

Figure 1. a) Structurally relevant interproton distances measured in streptomycin at 318 K and pH 7.0. b) Selective 1D NOE experiments with the 1D-DPFGSE NOE pulse sequence corresponding to the inversion of $H1_{Strp}$, $H1_{Glc}$ and $H2_{Glc}$ (from top to bottom). A one-dimensional spectrum of streptomycin is shown in the upper part of the figure.

Table 1. Experimentally measured and theoretically calculated distances and coupling constant values obtained for streptomycin in the free state. The conformational behaviour of this ligand was found to be basically independent of the pH in the 7.0–8.0 range. Unrestrained simulations (MD in the table) were carried out with explicit solvent, periodic boundary conditions (PBCs) and Ewald sums for the treatment of electrostatic interactions (see the Experimental Section). In vacuo MD-tar runs were performed with $\varepsilon = 80$. Experimentally derived distances for the protein-bound state, obtained from the analysis of TR-NOESY experiments at pH 7.0 are also shown. The corresponding values at pH 8.0 are shown in brackets only when they differ from those measured at pH 7.0, as in the case of $H2_{Strp}$–$H5_{Glc}$.

	Streptomycin			
d(A)	free	MD	Mdtar	bound
$H2_{Strp}$–$H3'_{Strp}$	2.5–2.7	2.4	2.5	2.7–3.0
$H4_{Strp}$–$H3'_{Strp}$	2.4–2.6	2.4	2.5	2.7–3.0
$H1_{Strp}$–$H4_{Strn}$	<2.3	2.4	2.5	<2.3
$H2_{Strp}$–$H4_{Strn}$	3.0–3.2	4.2	3.4	>3.8
$H4_{Strp}$–$H4_{Strn}$	3.1–3.3	4.6	3.5	>3.8
$H1_{Strp}$–$H1_{Glc}$	3.2–3.8	3.6	3.4	3.0–3.5
$H1_{Strp}$–$H5_{Glc}$	2.5–2.7	2.6	2.6	2.4–2.6
$H2_{Strp}$–$H1_{Glc}$	2.3–2.5	2.3	2.4	2.2–2.4
$H2_{Strp}$–$H5_{Glc}$	2.9–3.1	4.2	3.2	>3.6 (>3.7)
$H2_{Strp}$–Me_{Glc}	3.8–4.8	4.0	4.1	3.5–4.5
$H3'_{Strp}$–Me_{Glc}	>4.0	4.5	5.2	>4.0
$H3'_{Strp}$–$H1_{Glc}$	-	4.0	4.1	>3.7
$H2_{Strp}$–$H4_{Strp}$	2.8–3.1	2.6	2.9	<2.6
J [Hz]	free	MD	Mdtar2	bound
$H1_{Strp}$–$H2_{Strp}$	<2.5	4.7	2.7	not available

A/A′ ($\phi/\psi_{Strp/Strn}$ $55\pm10/25\pm10$, $\phi/\psi_{Glc/Strp}$ $55\pm10/45\pm10$) and B/B′ ($\phi/\psi_{Strp/Strn}$ $30\pm10/-50\pm10$, $\phi/\psi_{Glc/Strp}$ $30\pm10/-60\pm10$) in Figure 2b, with relative populations around 40–45%, and 50–60%, respectively.

- An additional minor population around minimum C/B′ (Figure 2a), characterised by an "anti" (180°) orientation of ϕ_{Strp} is also detected. In fact, the presence of a certain population (<4%) around this conformational region is essential for correct reproduction of the $H2_{Strp}$–$H4_{Strn}$ and $H4_{Strp}$–$H4_{Strn}$ NOEs.
- According to the *J* values, the streptidine and the glucose rings adopt the $^4C_1$ and $^1C_4$ conformations, respectively.
- The furanose ring of streptose is rather flexible, presenting two different populations, with puckering values in the 100–175° and 210–300° ranges (see Figure S4a in the Supporting Information). Nevertheless, this conformational variability has only a limited effect on the global shape of the molecule. In fact, the $H1_{Strp}$-$C1_{Strp}$-$C2_{Strp}$-$H2_{Strp}$ dihedral angle (which has a large influence on the relative orientation of the Strn and Glc units) remains restricted for most of the time in the 90–140° range, as deduced from the NOE data and, especially, in agreement with the observed low $J_{H1,H2}$ value.
- The streptose side chain is >95% in the hydrated form, as previously observed by other authors.[23] The presence of strong intraresidue (d<2.6 Å) NOEs between $H3'_{Strp}$ and both $H2_{Strp}$ and $H4_{Strp}$ is consistent with an antiperiplanar orientation of $OH3_{Strp}$ with respect to $H3'_{Strp}$. This conclusion is in agreement with the operation of a *gauche* effect (Figure S4b).[24]

The bound state—molecular recognition of streptomycin by ANT (6): As a first step, a preliminary characterization of the protein and its interaction with ANT(6) was performed. Analytical ultracentrifugation experiments were carried out at different protein concentrations in the 1–20 μM range. The obtained results unambiguously show that ANT(6) is

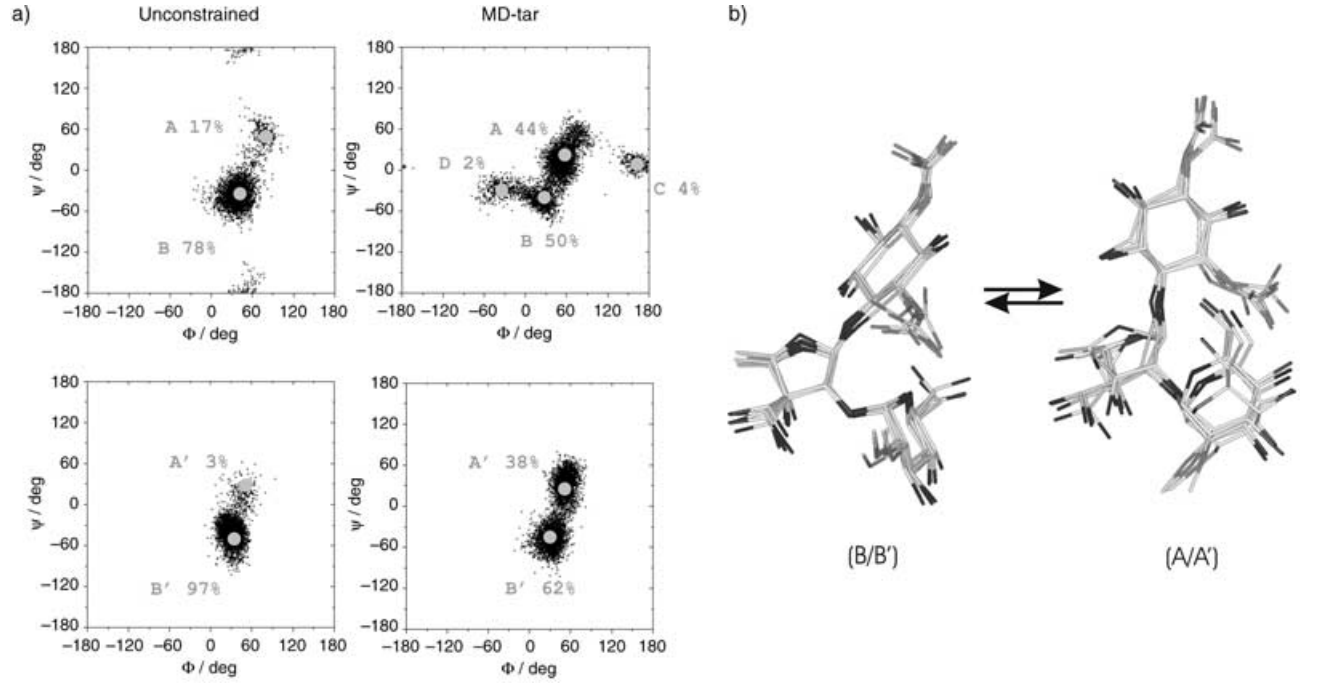

Figure 2. a) Left: Distributions obtained from a 20 ns unrestrained MD simulation for the Strp/Strn (top) and Glc/Strp (bottom) linkages with use of periodic boundary conditions, counter-ions and Ewald sums for the treatment of the electrostatic interactions. Right: Experimentally derived MD-tar distributions obtained from an 80 ns simulation for the Strp/Strn (top) and Glc/Strp (bottom) linkages with 13 distances and one *J* value. b) Schematic representations of the two main conformational families (A/A′ and B/B′) of streptomycin present in solution according to our combined NMR and MD analysis.

dimeric under all the experimental conditions tested. In addition, it binds one streptomycin molecule per monomer, with an apparent affinity defined by a binding constant $K_a = 5\times10^4\,\text{M}^{-1}$, according to preliminary ITC experiments at pH 7.5. A detailed thermodynamic characterization of the aminoglycoside–enzyme interaction is currently underway. These data suggest that ANT(6) might present structural similarities with *Staphylococcus aureus* ANT(4)[25] (a dimeric enzyme with a 30% identity with ANT(6)), for which the presence of two identical aminoglycoside and ATP binding sites per dimer has been shown by X-ray crystallography. In fact, association constants of the same order ($3–7\times10^4\,\text{M}^{-1}$) have been measured for ANT(4) with different aminoglycosides by our group (unpublished results).

NMR analysis of the structure of the protein-bound antibiotic: Upon binding to a receptor protein, flexible carbohydrate ligands are usually fixed in a specific bioactive conformation. In most cases this corresponds to one of the energy minima most populated in the free state. This cannot be regarded as a general rule, however, and several cases in which high-energy conformers are stabilised upon binding to a protein have been reported in recent years.[15] The conformational analysis of streptomycin shown above has conclusively demonstrated that this pseudotrisaccharide is rather flexible in solution. In fact, two major conformations are detected for both glycosidic linkages. This observation raises the question of which of these conformations (if either) is recognised by the enzyme ANT(6). In order to determine the bound structure of streptomycin, TR-NOESY experiments were carried out in the presence of ANT(6). TR-ROESY experiments were also performed to account for spin diffusion effects. In all cases, the enzyme activity was verified prior to and after the collection of the NMR data.

As a first step, different experimental conditions, including different temperatures and ligand to protein ratios, were tested. The best results were obtained at 308 K and at streptomycin/ANT(6) ratios of 20:1 to 30:1. TR-NOESY experiments were performed at pH 7.0 and 8.0, both at 500 and 600 MHz. Under all these sets of conditions, clear *negative* TR-NOEs (transferred nuclear Overhauser effects) were detected for the antibiotic. Interestingly, TR-NOE intensities measured at pH 8.0 were significantly larger than those measured at pH 7.0 (for instance, $\sigma_{\text{H1Glc–H2Glc}}(\text{pH 8})/\sigma_{\text{H1Glc–H2Glc}}(\text{pH 7}) = 5.0$), suggesting a larger rate constant k_{-1} at the former pH value, probably due to partial deprotonation of the glucose amino group at high pH, with a concomitant decrease in binding affinity. A full matrix relaxation analysis (in the presence of exchange) of the TR-NOE intensities with mixing time suggested that the off-rate constant is between 50 and 200 s^{-1}.

Under the same experimental conditions (500 MHz and 308 K), *positive* NOEs, albeit too weak for quantitative analysis, were measured for the ligand in the absence of the enzyme. As mentioned above, the collection of the data for the conformational analysis in the free state was performed

at 500 MHz and 318 K. For purposes of comparison, 2D-NOESY experiments were performed for the free antibiotic at both pH 7.0 and pH 8.0, but at a lower temperature of 278 K. At this temperature the antibiotic presented negative NOEs. Close inspection of these data sets shows that the conformational behaviour of streptomycin under these conditions is basically identical to that described above at pH 7.0 and 318 K.

To provide quantitative information about the ligand's protein-bound structure, NOE build-up curves were obtained from analysis of TR-NOESY experiments at different mixing times. Interproton distances (Table 1) were derived from the initial slopes as described in the Experimental Section. The ratios between the structurally relevant cross-relaxation rates and those corresponding to known fixed distances (used as references) in the free and protein-bound antibiotic are shown in Table 2 (at pH 8.0). Several conclusions can be drawn from these data:

- Firstly, strong $H1_{Glc}$–$H2_{Strp}$, $H5_{Glc}$–$H1_{Strp}$, and $H1_{Strp}$–$H4_{Strn}$ TR-NOEs were observed at every mixing time both at pH 7.0 and at pH 8.0 (see Figure 3a and Figure S5 in the Supporting Information). The distances derived from the corresponding NOE build-up curves are shown in Table 1. These values are fully consistent with a bound structure close to the B/B′ minimum for the antibiotic.
- The $H2_{Strp}$–$H5_{Glc}$ NOE, characteristic of the A/A′ minimum (present in the free state with an estimated population of 40–45%), was below the noise level in all the TR-NOESY experiments performed at pH 7.0. Although no precise value could be determined for this interproton distance in the antibiotic bound state, a lower limit

Table 2. Experimentally determined ratios between the structurally relevant cross-relaxation rates and those corresponding to known fixed distances for both the free and ANT(6)-bound streptomycin at pH 8.0. Fixed distances between $H1_{Glc}$–$H2_{Glc}$, $H1_{Glc}$–$H5_{Glc}$, $H1_{Strp}$–$H2_{Strp}$ and $H1_{Strp}$–$H4_{Strp}$ proton pairs are 2.4, 3.7, 2.9 and 3.7 Å respectively. The $H2_{Strp}$–$H5_{Glc}$ distance significantly increases in the bound state, with concomitant decreases in both the $H2_{Strp}$–$H4_{Strp}$ and the $H1_{Strp}$–$Me4_{Strp}$ distances upon binding, unequivocally indicating a shift in the conformational equilibrium.

σ ratio	Free 278 K	Bound 308 K
H1Glc–H2Strp/H1Glc–H2Glc	1.0	1.2
H1Strp–H4Strn/H1Strp–H2Strp	6.5	7.2
H1Strp–H5Glc/H1Strp–H2Strp	1.7	2.5
H2Strp–H5Glc/H2Strp–H1Strp	0.7	0.3
H5Glc–H2Strp/H5Glc–H1Glc	3.2	1.0
H2Strp–H4Strp/H2Strp–H1Strp	0.9	2.9
H1Strp–Me4Strp/H1Strp–H4Strp	0.4	1.1

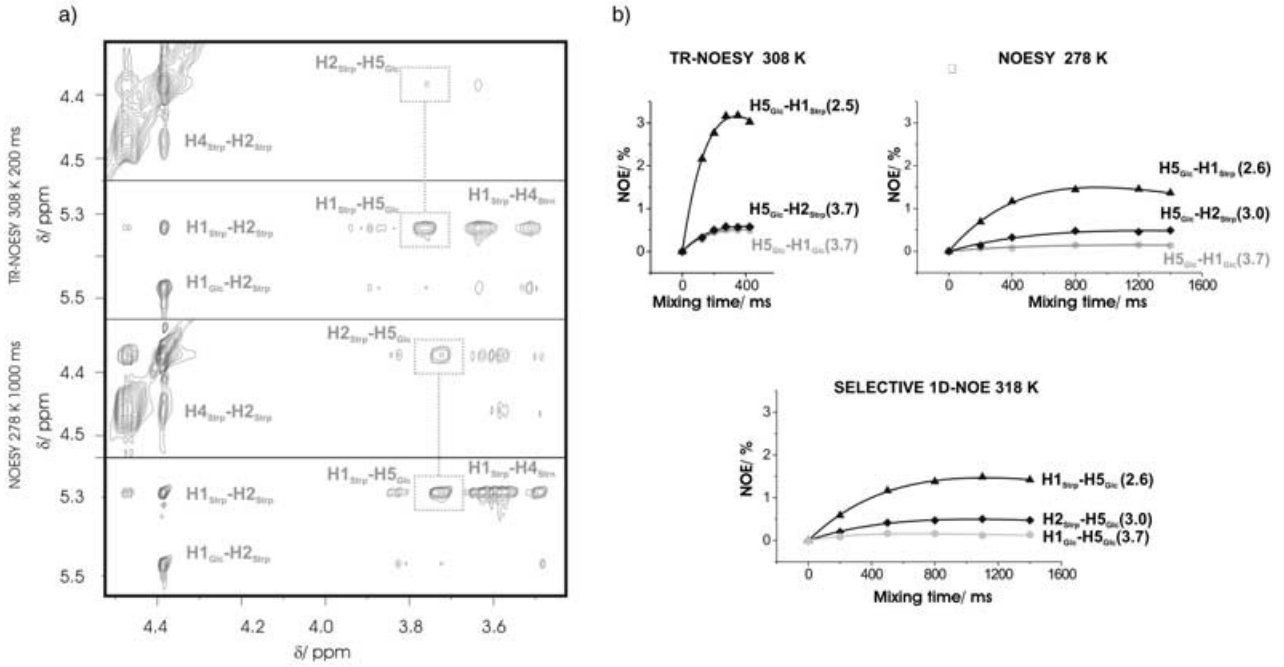

Figure 3. a) Two regions of 2D-NOESY spectra at pH 8.0 in the presence (two upper panels) and in the absence (two lower panels) of ANT(6). Large $H1_{Strp}$–$H5_{Glc}$ and $H2_{Strp}$–$H5_{Glc}$ NOEs, representative of the B/B′ and A/A′ conformational populations, respectively, are observed for the free antibiotic. In the presence of the enzyme, the $H2_{Strp}$–$H5_{Glc}$ NOE is extremely weak, indicating the shifting of the conformational equilibrium towards the B/B′ family. 2D TR-NOESY spectra for streptomycin in the presence of ANT(6) were performed at 308 K and a 20:1 ligand/protein ratio. However, 2D-NOESY spectra for the free antibiotic were performed at 278 K, due to the basically zero intensities of the NOE cross-peaks at 308 K. All the structurally relevant NOEs are labelled in grey. b) NOE build-up curves corresponding to $H5_{Glc}$–$H1_{Strp}$ and $H5_{Glc}$–$H2_{Strp}$ cross-peaks both in the presence (left) and in the absence (right) of the enzyme. The NOE-derived distances are shown in brackets. The build-up curve measured for the reference and $H5_{Glc}$–$H1_{Glc}$ cross-peak (corresponding to a distance of 3.7 Å) is shown in grey. In addition, the $H1_{Strp}$–$H5_{Glc}$, $H2_{Strp}$–$H5_{Glc}$ and $H1_{Glc}$–$H5_{Glc}$ NOE build-up curves obtained at 318 K from the analysis of selective 1D-NOE experiments are shown at the bottom of the figure. Notice that in this case the diagonal peak employed to normalize the NOE data is not $H5_{Glc}$ (this proton cannot be selectively inverted due to its close proximity to several other signals).

was estimated. For this purpose the $H2_{Strp}$–$H1_{Strp}$ cross-peak (corresponding to a distance between 2.8 and 3 Å independently of the furanose conformation) was used as reference. Taking the signal to noise ratio of the measured spectra into account it can be deduced that $\sigma_{H2Strp-H5Glc}/\sigma_{H2Strp-H1Strp} < 0.2$. The corresponding value for the free antibiotic was 0.7. According to these data, the average $H2_{Strp}$–$H5_{Glc}$ distance in the ANT(6)-bound streptomycin has to be greater than 3.6 Å. At pH 8.0, an extremely weak $H2_{Strp}$–$H5_{Glc}$ NOE could be detected (Figure 3). Its relative intensity is significantly reduced in comparison with that observed in the absence of the protein (for a comparison see Figure 3). With the $H2_{Strp}$–$H1_{Strp}$ and $H5_{Glc}$–$H1_{Glc}$ cross-peaks (see Table 2) as references, it can be shown that $\sigma_{H2Strp-H5Glc}/\sigma_{H2Strp-H1Strp} = 0.3$ and $\sigma_{H5Glc-H2Strp}/\sigma_{H5Glc-H1Glc} = 1$, which is in agreement with a $H2_{Strp}$–$H5_{Glc}$ distance of around 3.7 Å. In conclusion, the conformational behaviour of the streptomycin is clearly altered upon binding to ANT(6), with the A/A′ minimum either being unpopulated in the antibiotic protein-bound state or possibly exhibiting a very minor population.

- Similarly, the $H2_{Strp}$–$H4_{Strn}$ and $H4_{Strp}$–$H4_{Strn}$ cross-peaks representative of the minor (<5%) conformation—C/B′—were below the noise level in all the TR-NOESY spectra performed at pH 7.0. At pH 8.0, very weak NOEs were detected, although these signals were not present in the TR-ROESY spectra performed under identical conditions. All these data indicate that the enzyme does not recognize this conformer.
- A detailed conformational description of the streptose sugar unit in the bound state is hampered by the reduced amount of available experimental information (only a few NOEs). However, it is important to note that the most important structural parameter for the streptose ring, in terms of the antibiotic global shape, is the H1-C1-C2-H2 dihedral angle, which contributes to define the relative orientation of the streptidine and glucose moieties. As shown above, this angle was within the 90°–140° range for the free antibiotic. However, experimental evidence distinctly indicates that it has a larger value in the protein-bound state. Firstly, weak TR-NOE and TR-ROE cross-peaks (corresponding to distances of 3.5–4.0 Å) were observed between the $H1_{Glc}$–$H4_{Strn}$ (see Figure S6 in the Supporting Information) and $H6_{Glc}$–$H4_{Strn}$ proton pairs. These contacts, between the nonvicinal glucose and streptidine rings, are only compatible with a H1-C1-C2-H2 dihedral angle in the 150–180° range (for lower values, and for any low-energy orientation of the two glycosidic linkages, both distances are >4.5 Å). Secondly, at pH 8.0 (overlap between $H2_{Strp}$ and $H4_{Strp}$ makes it impossible to measure the $H2_{Strp}$–$H4_{Strp}$ NOE at pH 7.0), the $\sigma_{H2Strp-H4Strp}/\sigma_{H2Strp-H1Strp}$ ratio is significantly increased in the presence of ANT(6) (2.9 vs. 0.9 in the absence of the protein), which indicates that the $H2_{Strp}$–$H4_{Strp}$ distance is below 2.6 Å for the bound ligand (Figures 4a and and Figure S7 in the Supporting Information). This distance is only compatible with a near pseudoaxial orientation of both $H4_{Strp}$ and $H2_{Strp}$. Finally, the $H1_{Strp}$–$Me4_{Strp}$ distance is also reduced as a consequence of the ligand binding to ANT(6). Indeed, the $\sigma_{H1Strp-Me4Strp}/\sigma_{H1Strp-H4Strp}$ ratio increases from 0.4 in the absence of the protein to 1.1. This observation also suggests a pseudoaxial orientation of $H1_{Strp}$.

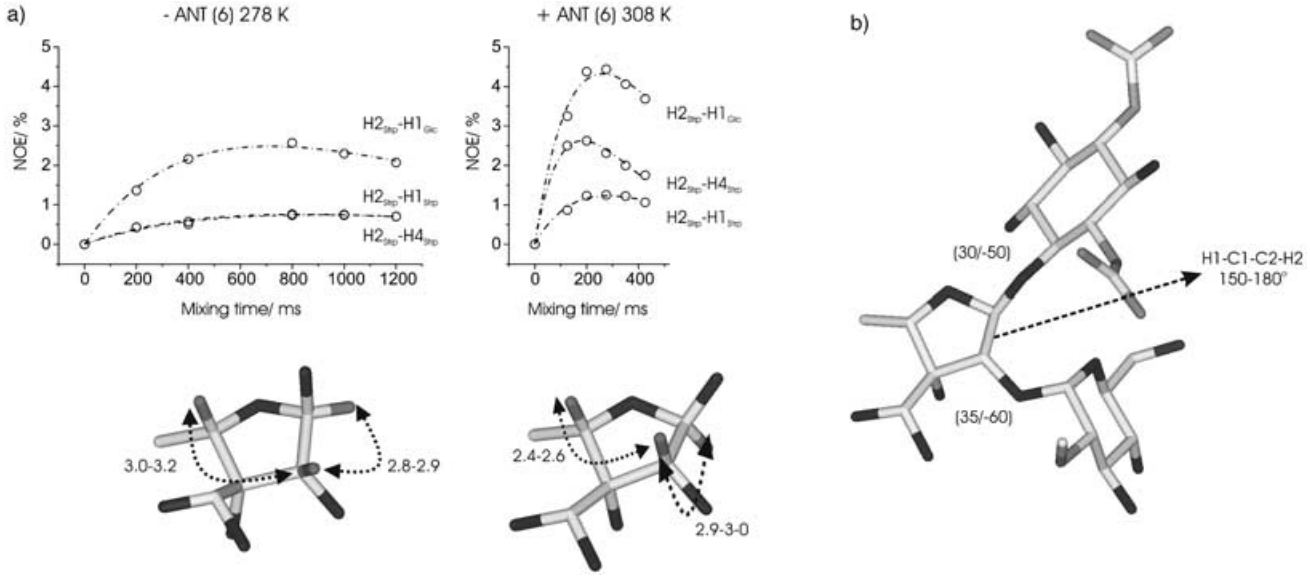

Figure 4. a) Top: NOE build-up curves corresponding to $H2_{Strp}$–$H1_{Strp}$, $H2_{Strp}$–$H4_{Strp}$ and $H2_{Strp}$–$H1_{Glc}$ cross-peaks both in the presence (right) and in the absence (left) of the enzyme. The increase in the $\sigma_{H2Strp-H4Strp}/\sigma_{H2Strp-H1Strp}$ ratio in the presence of ANT(6) is evident. Bottom: Average $H2_{Strp}$–$H4_{Strp}$ and $H2_{Strp}$–$H1_{Strp}$ distances in the free (left) and streptomycin protein-bound (right) state. The shortening of the $H2_{Strp}$–$H4_{Strp}$ distance upon binding to ANT(6) is consistent with a pseudoaxial orientation of both $H2_{Strp}$ and $H4_{Strp}$ in the antibiotic protein-bound state. Protons $H2_{Strp}$, $H4_{Strp}$ and $H1_{Strp}$ are shown in grey; oxygen atoms are represented in black. b) Schematic representation of the streptomycin ANT(6)-bound structure.

In conclusion, all these data indicate that the H1-C1-C2-H2 dihedral angle is shifted to higher values (150–180°) in the antibiotic ANT(6)-bound state with respect to that present in the free streptomycin.

Figure 4b shows an NMR-derived model for the ANT(6)-bound streptomycin. As would be expected, the conformational flexibility of this ligand is strongly reduced upon binding to the enzyme. In fact, the conformation selected by ANT(6), defined by ϕ/ψ Strp–Strn 30/−54, and ϕ/ψ Glc–Strp 33/−64, is close to the B/B′ geometry present in the free state, which showed a 50–60% population. The experimentally detected freezing of the ligand upon binding to ANT(6) would be expected to make a significant contribution to the global ΔS. The result is also relevant for the design of ANT (**6**) inhibitors.

Structural features of the interaction—NMR determination of the antibiotic recognition epitope: Saturation transfer difference experiments (STD-NMR) were performed to provide additional information regarding the antibiotic mode of binding to *Bacillus subtilis* ANT(6). Recent studies have shown that this NMR technique can be used for epitope mapping of the ligand.[26] In a typical STD experiment, the resonances of the protein are selectively saturated over a period of time, giving rise to intermolecular NOE effects with a weakly bound ligand. Identification of the ligand signals affected most strongly by saturation transfer from the protein permits the determination of which ligand protons are in close contact with the protein binding site and, therefore, constitute the recognition epitope. Figure 5a shows a one-dimensional spectrum of streptomycin together with a STD experiment corresponding to the antibiotic in the presence of ANT(6). The relative STD effects for streptomycin are shown in Figure 5b, mapped on the bioactive conformation of the antibiotic, as deduced from the TR-NOE experiments described above. They were normalised with the aid of the largest STD effect (the H3′ proton corresponding to the streptose unit, 100%). Clear differences between the different streptomycin protons can be observed. Thus, the largest intermolecular NOE corresponds to $H3'_{Strp}$. In addition, significant saturation transfer is also detected for Me_{Strp}, $H4_{Strp}$, $H2_{Strp}$ and $H1_{Glc}$. As observed in Figure 5b, all these protons are clustered around the same antibiotic region. In contrast, weak intermolecular NOEs were measured for $H3_{Glc}$, $H4_{Glc}$, $H5_{Glc}$ and $H6_{Glc}$, suggesting weak interaction between this streptomycin region and ANT(6). Although the strong overlap of proton signals in the streptidine unit prevents accurate quantification of STD signals, a magnetization transfer $>60\%$ was observed for protons H1 and H6. This observation is not surprising as position 6 in this unit is the one modified by the enzyme and so should be deeply buried in its binding pocket.

Specificity of the enzyme–aminoglycoside interaction: In order to check the ANT(6) specificity, the enzyme activity was tested with different aminoglycosides, including streptomycin, neomycin-B, kanamycin and spectinomycin (Scheme 2). The antibiotic adenylation can easily be monitored by ^{1}H NMR spectroscopy; the proton located on the same carbon as the OH modified by the enzyme is clearly shifted downfield as a result of this process. Enzymatic reactions were therefore carried out in NMR tubes. NMR spectra (including TOCSY and HMQC experiments) of the different antibiotics in the presence of equimolar amounts of ATP were recorded before and 4 h after addition of ANT(6) (5 μM). As would be expected, the enzyme is highly specific for streptomycin (no reaction was detected in any other case). In a second step, TR-NOESY experiments were carried out with neomycin and spectinomycin. Surprisingly, negative NOE cross-peaks were observed for both antibiotics in the presence of ANT(6) (see Figure S8a in the Supporting Information, protein/ligand ratio 1:20). In contrast,

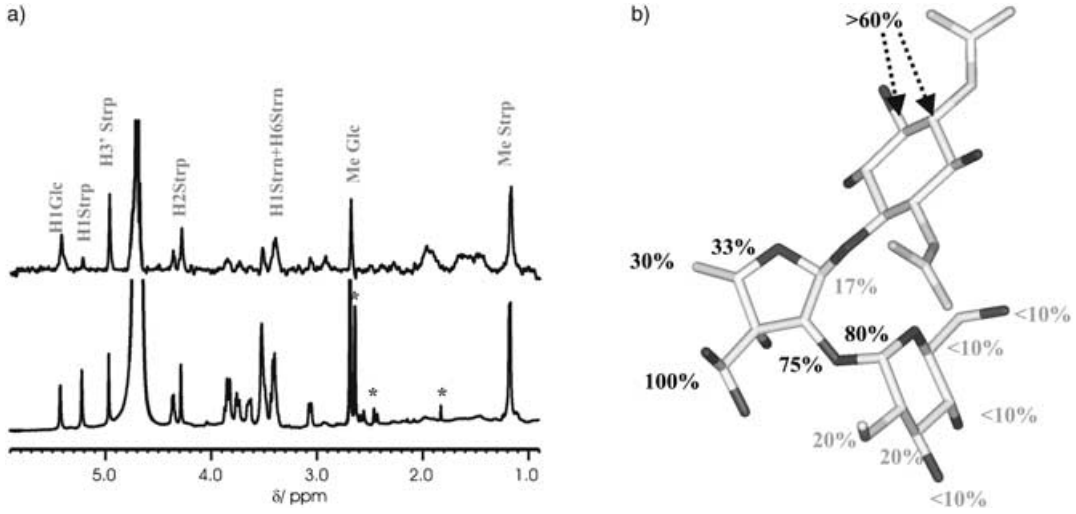

Figure 5. a) One-dimensional STD NMR (500 MHz) spectrum for streptomycin in the presence of ANT(6), together with the corresponding ^{1}H NMR reference spectrum. b) Relative STD effects for streptomycin bound to ANT(6).

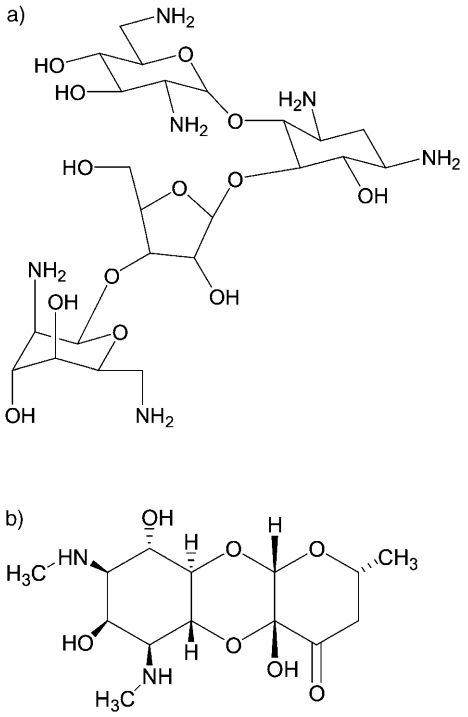

Scheme 2. Neomycin-B (a) and spectinomycin (b).

both ligands presented weak positive NOEs at 500 MHz in the absence of the enzyme. This observation clearly indicates that both aminoglycosides bind to ANT(6).

Finally, STD experiments for neomycin-B and spectinomycin were carried out (see Figure S8b in the Supporting Information). Clear magnetization transfer was observed for spectinomycin. In contrast, no STD signals were observed for neomycin-B under any conditions tested. To check the protein integrity, streptomycin was added to the NMR tube and the STD experiments were repeated. In this situation, clear STD signals were detected for streptomycin, but not for neomycin-B (see Figure S9 in the Supporting Information), indicating that neomycin-B is not deeply buried in the protein binding site. It appears probable that the presence of the streptidine ring (common to both streptomycin and spectinomycin but not present in neomycin-B) is essential for a better fitting of the ligand into the binding pocket.

In conclusion, although ANT(6) specifically modifies streptomycin, it is still able to interact with different aminoglycosides, probably in an unspecific manner, as shown by TR-NOESY experiments. The low sensitivity exhibited by this enzyme to the particular three-dimensional structure of the ligand strongly suggests that the aminoglycoside's unspecific binding is driven by electrostatic forces, similar to those that mediate the unspecific binding of aminoglycosides to DNA or RNA. This finding is consistent with the presence of a large negative electrostatic potential in the enzyme binding site. In fact, a highly negative potential has been observed for other aminoglycoside-modifying enzymes.[3] It seems clear from these data that both proteins and nucleic acids have a common strategy for the molecular recognition of these antibiotics.

The role of the nucleotide—structural features of the interaction between the nucleotide and ANT(6): To provide information about the nucleotide recognition process by ANT(6), STD and TR-NOE/TR-ROE experiments were also carried out for these ligands. No TR-NOEs were detected for ATP in the presence of the enzyme (ATP/enzyme 20:1). In contrast, strong negative NOEs were measured for AMP (AMP/enzyme 20:1). Interestingly, these TR-NOE cross-peaks disappear when ATP is added to the sample (ATP/AMP/enzyme 20:20:1). This observation clearly indicates that the enzyme has a higher affinity for ATP than for AMP and, therefore, that the triphosphate moiety makes a significant contribution to the stability of the complex. Despite this difference in affinity, STD experiments suggest a very similar binding mode for both ligands. Figure 6a shows one-dimensional spectra of AMP/ANT(6) (20:1) and ATP/ANT(6) (20:1) mixtures, together with the corresponding STD experiments. The relative STD effects for AMP/ATP, normalised to the largest STD effect, are shown in Fig-

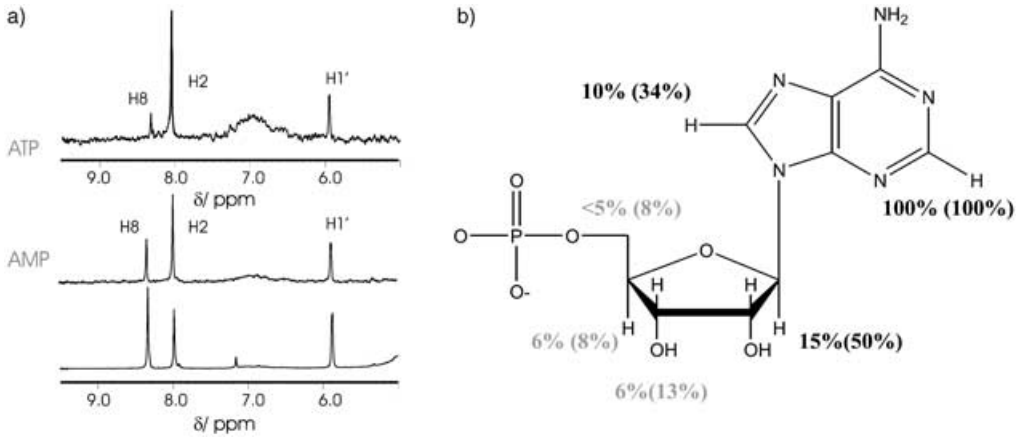

Figure 6. a) One-dimensional STD NMR (500 MHz) spectrum for ATP and AMP in the presence of ANT(6), together with the corresponding ^{1}H NMR reference spectra. b) Relative STD effects for ATP and AMP (in brackets) bound to ANT(6).

ure 6b. According to the STD and TR-NOE data, two ligand regions—the triphosphate moiety and the adenine ring—seem to play a role in the binding process.

The observed TR-NOE patterns for AMP (Figure 7, medium H8–H2′, medium H8–H3′, medium-weak H8–H5′/H5″, weak H8–H1′, medium-weak H1′–H4′) were almost identical in the presence and in the absence of streptomycin, consistently with an *anti* orientation for the glycosidic torsion. In fact, very strong H8–H1′ and extremely weak (or unobserved) H8–H2′, H8–H3′ and H8–H5′/H5″ contacts would be expected for a *syn*-type arrangement. In addition, the intensities of the H1′–H4′, H8–H2′ and H8–H3′ NOEs rule out a puckering value around 90°. Indeed, this "*East*" region of the pseudorotational path is characterised by a very short H1′–H4′ distance.[27] Therefore, the experimental data suggest the presence of a mixture of the ribose low-energy C2-*endo* (characterised by a short H8–H2′ distance) and C3-*endo* (characterised by a short H8–H3′ distance) conformations[27] in the protein binding site.

The role of the nucleotide—specificity of the molecular recognition process: In order to check the specificity of the enzyme, STD experiments were also carried out with other nucleotides. Figure 8 shows a one-dimensional spectrum of a GTP/ATP/ANT(6) mixture (20:20:1), together with the corresponding STD experiment. It can be observed that the magnetization is transferred to both nucleotides with the same intensity. From this observation alone it can be concluded that the enzyme recognizes both ligands with similar affinity. In fact, the amount of transferred magnetization to the different ligand protons is also very similar in both cases, suggesting a unique binding mode.

Additional STD experiments were carried out with UTP and CTP. Weak magnetization transfer to the nucleotide was also observed in each case, indicating that these ligands are also recognised to some extent by ANT(6).

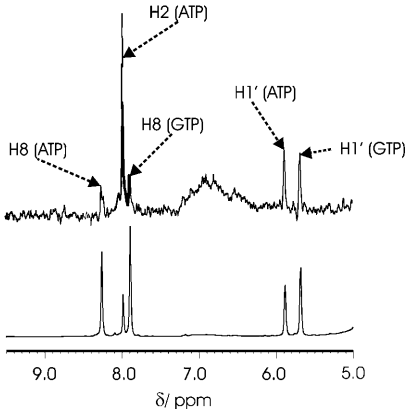

Figure 8. One-dimensional STD NMR (500 MHz) spectrum for an ATP/GTP mixture (1:1) in the presence of ANT(6), as well as the corresponding ^{1}H NMR reference spectra.

Finally, the enzyme activity was checked for the different nucleotide triphosphates. Figure 9a shows a region of the HSQC spectra corresponding to a GTP/streptomycin mixture before and after addition of ANT(6) (5 μM). It can be observed that, after a 2 h reaction period, the H6 proton of the streptidine unit is shifted downfield as a result of the nucleotide addition. An identical result was observed for ATP. The formation of the corresponding products was also confirmed by MALDI-TOF (molecular weights of 948.7 and 932.7 for the GMP-streptomycin and AMP-streptomycin sodium adducts, respectively). In contrast, no reaction was detected for UTP and CTP under identical conditions. The corresponding "nucleotidylated" antibiotics could only be obtained (and characterised by NMR and MALDI-TOF) after a 24 h reaction period with a high excess of 40 μM ANT(6) (molecular weights of 909.7 and 908.7 for UMP–streptomycin and CMP–streptomycin sodium adducts, respectively).

To analyse the enzyme specificity further, competition experiments were also performed. Figure 9b shows the evolution of an ATP/GTP/CTP/streptomycin mixture after addition of ANT(6) (5 μM). Interestingly, individual NMR signals can be observed for the H8 protons of adenine and guanine in the corresponding nucleotide triphosphates (ATP and GTP), and in the nucleotidylated streptomycin (AMP–streptomycin and GMP–streptomycin). Similarly, separate proton signals can be observed for the streptomycin

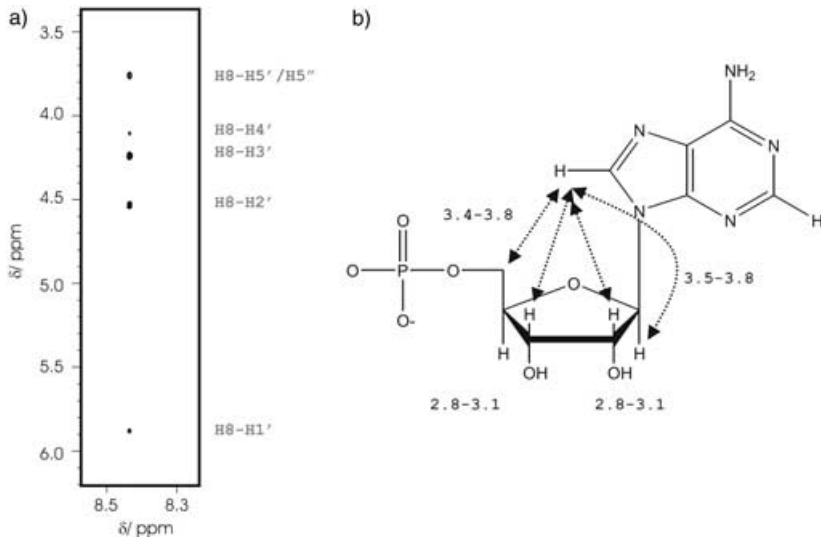

Figure 7. a) Region from a 200 ms TR-NOESY spectrum measured at 500 MHz, 298 K, pH 7.0 and 20:1 ligand/protein ratio. Negative NOES are observed for AMP. b) Schematic representation of AMP showing the key TR-NOEs. NOE-derived distances are also represented.

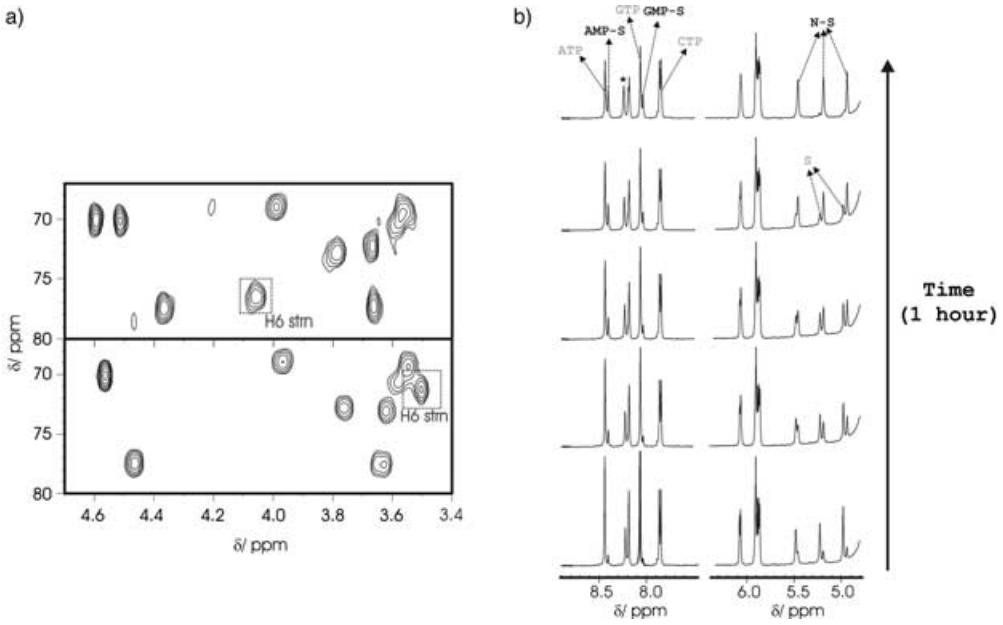

Figure 9. a) Region from a HSQC spectrum corresponding to a streptomycin/GTP mixture prior to (bottom) and 2 h after (top) addition of ANT(6) (5 μM). The downfield shifting of the streptidine H6 proton in the modified antibiotic is highlighted. b) Evolution of a ATP/GTP/CTP/streptomycin mixture after addition of ANT(6) (5 μM). Individual NMR signals can be observed for protons H8 of adenine and guanine in the corresponding nucleotide triphosphates (ATP and GTP, labelled in grey) and the nucleotidylated streptomycin (AMP-streptomycin and GMP-streptomycin, labelled as AMP-S and GMP-S in black). Similarly, separate proton signals can be observed for the streptomycin anomeric protons in the free and modified forms ("S" in the figure stands for streptomycin, "N-S" for nucleotidylated streptomycin). Signals from histidine present in the mixture as impurity are labelled with an asterisk (*).

anomeric protons in the free and modified forms. This allows an easy quantification of the reaction products. As shown in Figure 9b, after 1 h reaction time, the enzyme has modified all the streptomycin. Integration of the NMR signals corresponding to H8 of adenine and guanine in the nucleotidylated antibiotic shows that 55% of the product corresponds to AMP–streptomycin and 45% to the GMP derivative. Under these conditions, no reaction is observed for CTP, an observation confirmed by MALDI-TOF analysis of the reaction mixture. An identical result was obtained for UTP in similar competition experiments. According to all these data, *Bacillus subtilis* aminoglycoside-6-adenyl transferase shows a clear preference for nucleotide triphosphates incorporating purine aromatic systems (adenine or guanine). Although the enzyme retains its ability to recognize and modify CTP and UTP, these nucleotides are in general worse substrates than ATP or GTP.

Interestingly, the nucleotide conformation present in the ANT(6) binding site is rather different to that recognised by other aminoglycoside adenyltransferases such as ANT(4),[25] according to X-ray studies. In the latter case the glycosidic linkage adopts a "*syn*" orientation, in contrast with the "*anti*" orientation observed for ANT(6). In addition, most of the protein–nucleotide contacts in ANT(4) are localised around the sugar and the triphosphate backbone, and only a few of them involve the adenine ring. This could explain the low specificity exhibited by this enzyme for the nucleotide (in fact, GTP or UDP can also be employed by the enzyme for aminoglycoside nucleotidylation). In contrast, as mentioned above, ANT(6) shows a clear preference for nucleotides that include a purine system.

Conclusion

We have studied the structural and conformational features of the streptomycin interaction with *Bacillus subtilis* ANT(6), an enzyme involved in bacterial resistance against aminoglycoside antibiotics. The NMR data conclusively show that streptomycin is characterised by a high degree of flexibility in solution, with two major and several minor conformations in fast exchange. However, this equilibrium is clearly altered upon binding to ANT(6), and a single major population is present at the enzyme binding pocket. The molecular recognition process thus implies a conformational selection phenomenon.

In addition, the antibiotic recognition epitope has been analysed by STD-NMR experiments. The obtained data indicate that positions 2, 3 and 4 in the streptose unit, together with position 1 in the glucose ring and positions 1 and 6 in the streptidine moiety, are in close contact with the protein binding site. In contrast, positions 3–6 of the glucose unit are less affected upon saturation of the protein signals, suggesting a minor role for this antibiotic region in the recognition process.

From the enzyme perspective, surprisingly, although highly specific for streptomycin, ANT(6) is still able to recognize different aminoglycosides nonspecifically. This mo-

lecular recognition process is thus probably driven by electrostatic forces.

The structure of the nucleotide in the protein-bound state has also been analysed by TR-NOE/TR-ROE experiments. In this case, AMP is characterised by a glycosidic torsion angle in the "*anti*" range. In addition, the available experimental data are consistent with a mixture of *N* and *S* conformations in the bound state. Finally, STD and TR-NOE experiments suggest that the aromatic ring and the triphosphate moiety are both involved in contacts with the protein binding site. In fact, ANT(6) shows a clear specificity for nucleotides that incorporate a purine ring. The fine details of this interaction are rather different to those reported for other aminoglycoside adenyltransferases, such as ANT(4).[27]

Experimental Section

Cloning, expression and purification of ANT(6) was performed in our laboratory and will be described elsewhere. Streptomycin, ATP, CTP, GTP, UTP and the corresponding monophosphate derivatives were purchased from Sigma–Aldrich.

Calculations: Atomic charges were derived from HF/6–31G(d) RESP calculations, by use of the Gaussian 94[28] program. All MD simulations were carried out with the Sander module in the AMBER 5.0 package[21] and the Cornell et al. force field.[29] Parameters for the acetalic functions were taken from GLYCAM.[30] Unconstrained (in the presence of explicit TIP3P water and counter-ions) and MD-tar trajectories were carried out by a protocol identical to that described by Asensio et al.[18]

To calculate the antibiotic/ANT(6)-bound structure we employed a combined molecular dynamics/molecular mechanics protocol. Firstly, unrestrained 1 ns MD simulations were performed and streptomycin structures were saved every 100 ps. In a second step, the collected structures were subjected to a restrained energy minimization, with employment of TR-NOE-derived distances as experimental restraints.

NMR experiments: NMR experiments were recorded on Varian Unity 500, Bruker Avance 500, Bruker Avance 600 and Bruker Avance 800 spectrometers. For the analysis of the free antibiotic, selective 1D NOE experiments were carried out with the 1D-DPFGSE NOE pulse sequence at 318 K and pH 7.0. In addition, 2D-NOESY experiments were performed at pH 7.0 and 8.0 and at 278 K. For the TR-NOESY and TR-ROESY experiments, different experimental conditions were tested, including different temperatures, ligand to protein ratios and pH values. Best results were obtained at 308 K and at 20:1 to 30:1 ligand/ANT(6) ratio (protein concentration 75 μM), while the buffer conditions were sodium phosphate (20 mM), $MgCl_2$ (10 mM), pH 7.0–8.0. Additional experiments were performed in the absence of phosphate (proton signals in the streptidine ring presented greater dispersions under these conditions). Mixing times from 200 to 1400 ms and from 70 to 550 ms were employed for the analysis of the free and protein-bound states, respectively. NOE intensities were normalised with respect to the diagonal peak at 0 mixing time. Selective T_1 measurements were performed on the anomeric protons and several others to obtain the value discussed above. Experimentally measured NOEs were fitted to a double exponential function, $f(t) = p0(e^{-p2t})(1-e^{-p1t})$ with p0, p1 and p2 being adjustable parameters.[31] The initial slope was determined from the first derivative at time $t = 0$, $f(0) = p0p1$. Interproton distances were obtained from the initial slopes by employing the isolated spin pair approximation.

For TR-NOE/TR-ROE spectra, different ligand/enzyme ratios between 20:1 to 30:1 were employed. A variety of mixing times were employed for the TR-NOESY experiments. According to the estimated binding constant, K_a higher than $10^4\,M^{-1}$, the protein is saturated under the experimental conditions used. No T_2-filter or short spin lock pulse SL ($T_{1\rho}$-filter) was employed to remove the background protein signals. Nevertheless, TR-ROESY experiments were also carried out to detect and to exclude peaks due to spin diffusion effects. A continuous wave spin lock pulse was used during the 100 ms mixing time. Key NOEs were shown to be direct cross-peaks, since they showed different signs to diagonal peaks. In some cases these experiments allowed spin-diffusion effects to be identified. Since it is impossible to deduce the positions of the protons in the enzyme binding site accurately, only the protons of the ligand were considered for the relaxation matrix calculations, by the protocol employed by London,[32] as described.[15d] The overall correlation time τ_c for the free state was set to 0.30 ns and the τ_c for the bound state was estimated as 75 ns, according to the molecular weight of the enzyme ($\tau_c = 10^{-12}\ W_M$). To fit the experimental TR-NOE intensities, exchange rate constants between 50 and 1000 s^{-1}, and external relaxation times (ρ^*) for the bound state of 0.5, 1 and 2 s were tested. The best agreement was achieved by using $k = 50$–$200\ s^{-1}$ and $\rho^* = 1$ s.

Enzymatic reactions were performed in the NMR tubes. Equimolar amounts of the nucleotide triphosphate and the aminoglycoside were dissolved to a final concentration of 1.5 mM in buffer phosphate (20 mM, pH 7.0), $MgCl_2$ (10 mM). 2D DQF-COSY, TOCSY and HMQC spectra were recorded before and 2–4 h after addition of 5 μM ANT(6). The reaction products were additionally characterised by MALDI-TOF.

STD spectra were measured at different temperatures from 278 to 303 K with 6k (6144) scans. The reference spectra were measured with 3k (3072) scans. Saturation transfer was achieved by use of 40 selective Gaussian pulses (duration 50–10 ms, spacing 1 ms). A short 10 ms spin-lock pulse was employed to remove the background protein signals. The protein envelope was irradiated at $\delta = 0.5$ (on-resonance) and $\delta = 40$ (off-resonance). Subsequent subtraction was achieved by phase cycling.

Acknowledgements

Financial support from DGES (grants BQU2001–3693-C02–02 and BQU-2003–3550-C03–01) is acknowledged. F.C. thanks the Comunidad Autónoma de la Rioja for a postdoctoral fellowship. The authors thank CESGA (Santiago de Compostela) for computer support.

[1] D. Greenwood, in *Antimicrobial Chemotherapy* (Ed.: Greenwood), Oxford University Press, Oxford, **1995**, pp. 32–48.
[2] A. P. Carter, W. M. Clemons, D. E. Brodersen, R. J. Morgan-Warren, B. T. Wimberly, V. Ramakrishnan, *Nature* **2000**, *407*, 340–348.
[3] C. A. Smith, E. N. Baker, *Curr. Drug Targ. - Inf. Dis.* **2002**, *2*, 143–160.
[4] N. Honore, S. T. Cole, *Antimicrob. Agents Chemother.* **1994**, *38*, 238.
[5] J. Davies, G. D. Wright, *Trends Microbiol.* **1997**, *5*, 234.
[6] G. J. Alangaden, B. N. Kreiswirth, A. Aouad, M. Khetarpal, F. R. Igno, S. L. Moghazeh, E. K. Manavathu, A. Lerner, *Antimicrob. Agents Chemother.* **1998**, *42*, 1295.
[7] Y. Suzuki, C. Katsukawa, A. Tamaru, C. Abe, M. Makino, Y. Mizuguchi, H. Taniguchi, *J. Clin. Microbiol.* **1998**, *36*, 1220.
[8] E. A. DeStasio, D. Moazed, H. F. Noller, A. E. Dahlberg, *EMBO J.* **1989**, *8*, 1213.
[9] D. Fourmy, M. I. Recht, J. D. Puglisi, *J. Mol. Biol.* **1998**, *277*, 347–362.
[10] J. J. Rusthoven, T. A. Davies, S. A. Lerner, *Am. J. Med.* **1979**, *67*, 702.
[11] P. R. Langford, H. Anwar, I. Gonda, M. R. Brown, *FEMS Microbiol. Lett.* **1989**, *52*, 33.
[12] I. Phillips, K. Shannon, *Br. Med. Bull.* **1984**, *40*, 28.
[13] G. D. Wright, in *Bacterial Resistance to Antimicrobials* (Eds.: Lewis, Salyers, Taber, Wax), Marcel Dekker, New York, **2002**, pp. 91–121.
[14] *Glycosciences: Status and Perspectives*, (Eds.: H. J. Gabius, S. Gabius), Chapman & Hall, London, **1997**.
[15] a) J. F. Espinosa, J. Cañada, J. L. Asensio, H. Dietrich, M. Martín-Lomas, R. R. Schmidt, J. Jiménez-Barbero, *Angew. Chem.* **1996**, *108*, 323–326; *Angew. Chem. Int. Ed. Engl.* **1996**, *35*, 303–306; b) J. F.

Espinosa, E. Montero, A. Vian, J. Garcia, H. Dietrich, M. Martín-Lomas, R. R. Schmidt, A. Imberty, J. Cañada, J. Jiménez-Barbero, *J. Am. Chem. Soc.* **1998**, *120*, 10862–10871; c) M. J. Milton, D. R. Bundle, *J. Am. Chem. Soc.* **1998**, *120*, 10547–10548; d) A. Garcia, E. Montero, J. L. Muñoz, J. F. Espinosa, A. Vian, J. L. Asensio, F. J. Cañada, J. Jimenez-Barbero, *J. Am. Chem. Soc.* **2002**, *124*, 4804–4810.

[16] a) N. Noguchi, K. Ohmiya, P. Tanaka, K. O'hara, M. Kono, *Agric. Biol. Chem.* **1989**, *53*, 2519–2520; b) K. O'hara, K. Ohmiya, M. Kono, *Antimicrob. Agents Chemother.* **1988**, *32*, 949–950.

[17] S. W. Homans, *Biochemistry* **1990**, *29*, 9110–9118.

[18] J. L. Asensio, A. Hidalgo, I. Cuesta, C. González, J. Cañada, C. Vicent, J. L. Chiara, G. Cuevas, J. Jiménez-Barbero, *Chem. Eur. J.* **2002**, *8*, 5228–5240.

[19] T. Haselhorst, T. Weimar, T. Peters, *J. Am. Chem. Soc.* **2001**, *123*, 10705–10714.

[20] D. A. Pearlman, *J. Biomol. NMR* **1994**, *4*, 1–16.

[21] D. A. Pearlman, D. A. Case, J. W. Caldwell, W. S. Ross, T. E. Cheatham, S. DeBolt, D. Ferguson, G. Siebal, P. Kollman, *Comput. Phys. Commun.* **1995**, *91*, 1–41.

[22] M. Chiansan, N. A. Baner, J. Simpson, J. A. McCammon, *J. Am. Chem. Soc.* **2002**, *124*, 1438–1442.

[23] K. Bock, C. Pedersen, *J. Antibiot.* **1974**, 27, 139–140.

[24] a) G. R. C. Thatcher, *The anomeric effect and associated stereoelectronic effects*, American Chemical Society, Washington, D. C., **1993**. b) A. J. Kirby, *The anomeric effect and related stereoelectronic effects at oxygen*, Springer, Heidelberg, Germany, **1983**.

[25] L. C. Pedersen, M. M. Benning, M. H. Holden, *Biochemistry* **1995**, *34*, 13305.

[26] B. Meyer, T. Peters, *Angew. Chem.* **2003**, *115*, 890–918; *Angew. Chem. Int. Ed.* **2003**, *42*, 8, 865–889.

[27] A. N. Lane, *Conformation of nucleic acids: problems and solutions.* In ACS symposium series 682, Molecular modelling of nucleic acids (Eds.: N. B. Leontis, J. SantaLucia), **1998**, The American Chemical Society, Washington, D. C., USA.

[28] Gaussian 94, Revision D.4, M. J. Frisch, G. W. Trucks, H. B. Schlegel, P. M. W. Gill, B. G. Johnson, M. A. Robb, J. R. Cheeseman, T. Keith, G. A. Petersson, J. A. Montgomery, K. Raghavachari, M. A. Al-Laham, V. G. Zakrzewski, J. V. Ortiz, J. B. Foresman, J. Cioslowski, B. B. Stefanov, A. Nanayakkara, M. Challacombe, C. Y. Peng, P. Y. Ayala, W. Chen, M. W. Wong, J. L. Andres, E. S. Replogle, R. Gomperts, R. L. Martin, D. J. Fox, J. S. Binkley, D. J. Defrees, J. Baker, J. P. Stewart, M. Head-Gordon, C. Gonzalez, J. A. Pople, *Gaussian, Inc.*, Pittsburgh, PA, **1995**.

[29] W. D. Cornell, P. C. Cieplack, I. Bayly, I. R. Gould, K. Merz, D. M. Ferguson, D. C. Spellmeyer, T. Fox, J. W. Caldwell, P. A. Kollman, *J. Am. Chem. Soc.* **1995**, *117*, 5179.

[30] R. J. Woods, R. A. Dwek, C. J. Edge, D. Fraser-Reid, *J. Phys. Chem.* **1995**, *99*, 3832–3839.

[31] T. Haselhorst, T. Weimar, T. Peters, *J. Am. Chem. Soc.* **2001**, *123*, 10705–10714.

[32] R. E. London, M. E. Pearlman, D. G. Davis, *J. Magn. Reson.* **1992**, *97*, 79–87.

Received: September 14, 2004
Revised: April 17, 2005
Published online: June 28, 2005

